

**Observation of  
chemical  
modification of Asian  
Dust particles**

Young-Chul Song et al.

This discussion paper is/has been under review for the journal Atmospheric Chemistry and Physics (ACP). Please refer to the corresponding final paper in ACP if available.

# Observation of chemical modification of Asian Dust particles during long-range transport by the combined use of quantitative ED-EPMA and ATR-FT-IR imaging

**Young-Chul Song, Hyo-Jin Eom, Hae-Jin Jung, Md Abdul Malek, HyeKyeong Kim, and Chul-Un Ro**

Department of Chemistry, Inha University, 253, Yonghyun-dong, Nam-gu, Incheon 402-751, Korea

Received: 10 September 2012 – Accepted: 3 October 2012 – Published: 17 October 2012

Correspondence to: Chul-Un Ro (curo@inha.ac.kr)

Published by Copernicus Publications on behalf of the European Geosciences Union.

Title Page

Abstract

Introduction

Conclusions

References

Tables

Figures

⏪

⏩

◀

▶

Back

Close

Full Screen / Esc

Printer-friendly Version

Interactive Discussion

## Abstract

In our previous works, it was demonstrated that the combined use of quantitative energy-dispersive electron probe X-ray microanalysis (ED-EPMA), which is also known as low-Z particle EPMA, and attenuated total reflectance FT-IR (ATR-FT-IR) imaging has great potential for a detailed characterization of individual aerosol particles. In this study, individual Asian Dust particles collected during an Asian Dust storm event on 11 November 2011 in Korea were characterized by the combined use of low-Z particle EPMA and ATR-FT-IR imaging. The combined use of the two single-particle analytical techniques on the same individual particles showed that Asian Dust particles had experienced extensive chemical modification during long-range transport. Overall, 109 individual particles were classified into four particle types based on their morphology, elemental concentrations, and molecular species and/or functional groups of individual particles available from the two analytical techniques: Ca-containing (38 %); NaNO<sub>3</sub>-containing (30 %); silicate (22 %); and miscellaneous particles (10 %). Among the 41 Ca-containing particles, 10, 8, and 14 particles contained nitrate, sulfate, and both, respectively, whereas only two particles contained unreacted CaCO<sub>3</sub>. Airborne amorphous calcium carbonate (ACC) particles were observed in this Asian Dust sample for the first time, where their IR peaks for the insufficient symmetric environment of CO<sub>3</sub><sup>2-</sup> ions of ACC were clearly differentiated from those of crystalline CaCO<sub>3</sub>. This paper also reports the field observations of CaCl<sub>2</sub> particles converted from CaCO<sub>3</sub> for the Asian Dust sample collected in the planetary boundary layer. Thirty three particles contained NaNO<sub>3</sub>, which are the reaction products of sea-salt and NO<sub>x</sub>/HNO<sub>3</sub>, whereas no genuine sea-salt particles were encountered, indicating that sea-salt particles are more reactive than CaCO<sub>3</sub> particles. Some silicate particles were observed to contain nitrate, sulfate, and water. Among 24 silicate particles, 10 particles contained water, the presence of which could facilitate atmospheric heterogeneous reactions of silicate particles including swelling minerals, such as montmorillonite and vermiculite, and non-swelling ones, such as feldspar and quartz. This paper provides detailed information on

## Observation of chemical modification of Asian Dust particles

Young-Chul Song et al.

Title Page

Abstract

Introduction

Conclusions

References

Tables

Figures



Back

Close

Full Screen / Esc

Printer-friendly Version

Interactive Discussion



the physicochemical characteristics of individual Asian Dust particles that experienced extensive chemical modification during long-range transport through the combined use of the two single-particle analytical techniques.

## 1 Introduction

Nearly every spring, "Asian Dust" originating mostly in Central China's and Mongolia's arid areas is transported to eastern China, the industrialized regions of China, and over the Yellow Sea to Korea, Japan, and even the Pacific Ocean (Fairlie et al., 2007; Hwang et al., 2008; Uno et al., 2009; Geng et al., 2009). Asian Dust storms inject immense quantities of dust particles from arid and semiarid areas into the atmosphere and periodically contribute to the large global aerosol load. These particles can affect the radiative balance (Bergstrom et al., 2007), prevalence of ice nuclei and cloud condensation nuclei (Andreae and Rosenfeld, 2008; Manktelow et al., 2010), as well as the atmospheric deposition of nutrients and toxins (Baker et al., 2003; Paytan et al., 2009). Mineral dust particles provide reactive surfaces for heterogeneous reactions with trace atmospheric gases, leading to chemical modification of the particles that ultimately affects the atmospheric chemical balance and photochemical cycle (Price et al., 2004; Sullivan et al., 2007a). At the same time, modification of the physicochemical properties of particles can alter their optical properties as well as their direct and indirect radiative forcing (Li-Jones et al., 1998; Xu et al., 2004). Therefore, the atmospheric processing of Asian mineral dust during long range transport has attracted increasing attention (Huebert et al., 2003; Arimoto et al., 2004; Maxwell-Meier et al., 2004; McNaughton et al., 2004).

In our previous studies (Ro et al., 2005; Hwang and Ro, 2005, 2006; Hwang et al., 2008; Geng et al., 2009), Asian Dust particle samples collected in Korea during 10 dust storm events between 2000 and 2006 were examined using quantitative energy-dispersive electron probe X-ray microanalysis (ED-EPMA), named low-Z particle EPMA. Low-Z particle EPMA is a powerful single-particle analytical technique for

## Observation of chemical modification of Asian Dust particles

Young-Chul Song et al.

Title Page

Abstract

Introduction

Conclusions

References

Tables

Figures



Back

Close

Full Screen / Esc

Printer-friendly Version

Interactive Discussion



**Observation of  
chemical  
modification of Asian  
Dust particles**

Young-Chul Song et al.

Title Page

Abstract

Introduction

Conclusions

References

Tables

Figures

⏪

⏩

◀

▶

Back

Close

Full Screen / Esc

Printer-friendly Version

Interactive Discussion

the characterization of airborne aerosol particles, because the particle size distribution and quantitative chemical composition of individual particles can be obtained without a complicated sample pretreatment process. Moreover, many environmentally important atmospheric particles, e.g. sulfates, nitrates, ammonium, and carbonaceous species, have been elucidated at least semi-quantitatively by the application of this technique (Kim and Ro, 2010; Geng et al., 2010). Previous studies have shown that Asian Dust particles experience chemical modification when they pass through industrialized regions of China and over the Yellow Sea by entrained air pollutants and sea-salts, respectively (Ro et al., 2005; Hwang and Ro, 2005; Hwang et al., 2008). For all the Asian Dust particle samples investigated, the most abundant minerals were silicates, except for one sample collected on 11 November 2002, where Ca-containing particles were the most abundant (Hwang and Ro, 2005; Ro et al., 2005). This unique sample was again examined to obtain more detailed information on the chemical compositions and morphology of individual Asian Dust particles of the sample, and it appeared that the particles of the sample had experienced extensive chemical modification during long-range transport (Hwang et al., 2006). Among overall 178 analyzed particles, the number of reacted (aged) particles was 81, and heterogeneous chemical reactions occurred mostly on  $\text{CaCO}_3$  mineral dust (54 particles) and sea-salt (26 particles).

Nevertheless, low-Z particle EPMA has a limitation for the exact mineral speciation of silicate particles because their chemical compositions and crystal structures are so diverse that the elemental concentrations obtained from the X-ray spectra are not sufficient for mineral speciation. In many cases, airborne particles are internal mixtures of two or more chemical species, for which X-ray analysis is even more difficult. Recently, our group reported that various types of individual airborne particles could be identified clearly by the combined use of low-Z particle EPMA and attenuated total reflectance FT-IR (ATR-FT-IR) imaging, where both the elemental chemical composition and molecular species of the same individual particles can be obtained from their X-ray and ATR-FT-IR spectral data (Ryu and Ro, 2009; Jung et al., 2010; Song et al., 2010; Malek et al., 2011; Maskey et al., 2011). Low-Z particle EPMA and ATR-FT-IR imaging

can provide information on their morphology and elemental concentrations, as well as their molecular species, functional groups, crystal structure, and physical phase of the same individual particles, respectively. These two techniques provide complementary information because low-Z particle EPMA has a limitation on molecular speciation, particularly for the organic moiety, and ATR-FT-IR imaging is quite qualitative and has limited spatial resolution, resulting in a better understanding of the physicochemical characteristics of individual particles than when the techniques were used alone.

In this study, the Asian Dust sample collected on 11 November 2002 was examined to obtain detailed physicochemical characteristics of Asian Dust particles, which experienced extensive chemical modification during long-range transport, by the combined application of low-Z particle EPMA and ATR-FT-IR imaging. Overall, 109 individual particles were observed to be mainly Ca-containing, NaNO<sub>3</sub>-containing, and silicate particles, even though the internal mixing states of the individual particles were rather complicated.

## 2 Experimental section

### 2.1 Sample

On 11 November 2002 when an Asian Dust storm event occurred, aerosol particle samples were collected on the roof of a campus building of Hallym University located in Chuncheon, Korea. Chuncheon (37° 89' N, 127° 73' E) is a relatively small city (population: 0.26 million, area: 1116 km<sup>2</sup>) with a mostly rural character outside of the central district that is free of industrial complexes. This event was a record-breaking episode and was reported to originate from the Gobi and Inner Mongolian Deserts (Chung et al., 2003). The single particle analytical results from low-Z particle EPMA and more details on this sample can be found elsewhere (Ro et al., 2005; Hwang and Ro, 2005, 2006). Particles were sampled on Ag foil using a seven stage May cascade impactor. The May impactor has, at a 20 L min<sup>-1</sup> sampling flow, an aerodynamic cut off of 16,

## Observation of chemical modification of Asian Dust particles

Young-Chul Song et al.

Title Page

Abstract

Introduction

Conclusions

References

Tables

Figures

⏪

⏩

◀

▶

Back

Close

Full Screen / Esc

Printer-friendly Version

Interactive Discussion



8, 4, 2, 1, 0.5, and 0.25  $\mu\text{m}$  for stages #1–7, respectively. The samples were placed in plastic carriers, sealed, and stored in a desiccator. Overall, 109 particles for the stage 3 sample were analyzed in this study.

## 2.2 Low-Z particle EPMA

5 Low-Z particle EPMA was applied before the ATR-FT-IR imaging measurements to obtain morphological and elemental compositional information on the individual particles. The measurements were carried out using a Jeol JSM-6390 scanning electron microscope equipped with an Oxford Link SATW ultrathin window EDX detector. The resolution of the detector is 133 eV for Mn- $K\alpha$  X-rays. The X-ray spectra were recorded using  
10 Oxford INCA Energy software. An accelerating voltage of 10 kV was chosen to achieve the optimal experimental conditions, such as a low background level in the spectra and high sensitivity for low-Z element analysis. The beam current was 1.0 nA for all measurements. A more detailed discussion of the measurement conditions is reported elsewhere (Ro et al., 1999). The net X-ray intensities of the elements were obtained  
15 by a non-linear least-squares fitting of the collected spectra using the AXIL program (Vekemans et al., 1994). The elemental concentrations of the individual particles were determined from their X-ray intensities by the application of a Monte Carlo simulation combined with reverse successive approximations (Ro et al., 2003, 2004). The quantification procedure provided results accurate to within 12% of the relative deviations  
20 between the calculated and nominal elemental concentrations when the method was applied to various types of standard particles, such as NaCl,  $\text{Al}_2\text{O}_3$ ,  $\text{CaSO}_4 \cdot 2\text{H}_2\text{O}$ ,  $\text{Fe}_2\text{O}_3$ ,  $\text{CaCO}_3$ , and  $\text{KNO}_3$  (Ro et al., 2000, 2001). The low-Z particle EPMA method can provide quantitative information on the chemical composition of individual particles, and particles can be classified based on their chemical species.

### Observation of chemical modification of Asian Dust particles

Young-Chul Song et al.

Title Page

Abstract

Introduction

Conclusions

References

Tables

Figures

⏪

⏩

◀

▶

Back

Close

Full Screen / Esc

Printer-friendly Version

Interactive Discussion



### 2.3 ATR-FT-IR imaging technique

ATR-FT-IR imaging measurements were performed using a Perkin Elmer Spectrum 100 FT-IR spectrometer interfaced to a Spectrum Spotlight 400 FT-IR microscope. For ATR imaging, an ATR accessory employing a germanium hemispherical internal reflection element (IRE) crystal with a diameter of 600  $\mu\text{m}$  was used. The ATR accessory was mounted on the X-Y stage of the FT-IR microscope and the IRE crystal made contact with the sample via a force lever. The ultimate spatial resolution of the IR imaging is approximately equal to the wavelength of the incident IR radiation. On the other hand, the hemispherical IRE crystal acts like a lens in that the IR beam is condensed when the beam strikes the IRE. The extent of condensation is proportional to the refractive index of the IRE material (4.0 for germanium) (Griffiths and de Haseth, 2007). Therefore, a spatial resolution of 3.1  $\mu\text{m}$  at 1726  $\text{cm}^{-1}$  (5.79  $\mu\text{m}$ ) was achieved beyond the ultimate spatial resolution limit. A 16  $\times$  1 pixel Mercury Cadmium Telluride (MCT) array detector was used to obtain FT-IR images with a pixel size of 1.56  $\mu\text{m}$ . For each pixel, an ATR-FT-IR spectrum, ranging from 680 to 4000  $\text{cm}^{-1}$  with a spectral resolution of 8  $\text{cm}^{-1}$ , was obtained from eight interferograms, which were co-added and Fourier-transformed. The position of the crystal on the sample was determined using an optical microscope equipped with a light-emitting diode and charge-coupled device camera. The optical image was used to identify the same single particles that were analyzed using low-Z particle EPMA before ATR-FT-IR imaging because optical microscopy provides an image of sufficient spatial resolution to help locate the same image field observed by low-Z particle EPMA. Spectral data processing was performed using Perkin Elmer Spectrum IMAGE software, where the images were corrected for atmospheric effects and the spectral information at each pixel was extracted by principal component analysis (PCA). A more detailed description of ATR-FT-IR imaging can be found elsewhere (Ryu and Ro, 2009; Jung et al., 2010; Song et al., 2010; Malek et al., 2011).

## Observation of chemical modification of Asian Dust particles

Young-Chul Song et al.

Title Page

Abstract

Introduction

Conclusions

References

Tables

Figures

⏪

⏩

◀

▶

Back

Close

Full Screen / Esc

Printer-friendly Version

Interactive Discussion



### 3 Results and discussion

Figure 1 shows secondary electron image (SEI) obtained before the ATR-FT-IR imaging measurements (Fig. 1a), visible light optical image (Fig. 1b), ATR-FT-IR image (Fig. 1c), and SEI after ATR-FT-IR imaging (Fig. 1d) of the same 109 individual airborne Asian Dust particles on Ag foil. For the combined application of the two single-particle analytical techniques, the morphology and chemical compositions of all the particles on the image field were obtained by low-Z particle EPMA. Optical microscopy was used to locate the same image field for ATR-FT-IR imaging (Fig. 1b). After the relocation of the image field, the sample was placed in contact with the IRE crystal for the ATR-FT-IR imaging measurement. The ATR-FT-IR image (Fig. 1c) was obtained by PCA analysis after the first differentiation of the original ATR-FT-IR spectra at all of the pixels in the image. Although the qualities of the SEIs and ATR-FT-IR image differ due to the inherently different spatial resolutions of the images, the same patterns of particle location among the images ensured that the same micrometer sized particles were observed. Their equivalent diameters ranged from 1.5 to 14.0  $\mu\text{m}$  (determined from SEI obtained before the ATR-FT-IR imaging), where the equivalent diameter was calculated by assuming that a particle with the same area for a particle on SEI is circular. The area of each image was approximately  $300 \times 200 \mu\text{m}^2$ . The number of pixels for the ATR-FT-IR image is  $\sim 25\,000$  considering that the pixel size of the ATR-FT-IR image is  $1.56 \times 1.56 \mu\text{m}^2$ . All pixels in the image contained the full IR spectra ranging from 680 to  $4000 \text{ cm}^{-1}$ . Although the experimental ATR-FT-IR imaging data were obtained on a  $1.56 \times 1.56 \mu\text{m}^2$  pixel size, the manufacture's software interpolates the ATR-FT-IR imaging pixel data onto a display image, so that the display image appears better than real.

The SEIs (Fig. 1a and d) clearly show the morphology and locations of the 109 particles before and after the ATR-FT-IR imaging. For ATR-FT-IR imaging, the samples were placed in contact with the IRE crystal so that some force was applied to the sample during contact. When good contact was made and the sample was well pressed

## Observation of chemical modification of Asian Dust particles

Young-Chul Song et al.

Title Page

Abstract

Introduction

Conclusions

References

Tables

Figures



Back

Close

Full Screen / Esc

Printer-friendly Version

Interactive Discussion



against the IRE crystal, the particles were (partly or fully) embedded into the ductile Ag collecting foil. For example, some nonconducting mineral particles sitting on the Ag foil (e.g. particles #3, 8, 9, 35, 36, 39, 41, and 101) appeared bright because of the high secondary and backscattered electron (SE and BSE) yields of insulating particles (Fig. 1a), whereas the particles on the SEI taken after the FT-IR measurements appeared dark as electrons can flow from the embedded particles to the metallic foil, resulting in low SE and BSE yields (Fig. 1d) (Goldstein et al., 2003). Most particles in Fig. 1a appeared dark due to their lower BSE yield than that of the Ag foil, resulting from their lower average atomic number (Goldstein et al., 2003). Many particles (#13, 25, 32, and 62, to name a few) in Fig. 1d showed a faint, blurred shade, which is different from the original dark particles in Fig. 1a, after the force by the IRE crystal was applied to the particles during contact, suggesting that the dark particles in Fig. 1a contain water. A previous study showed that those dark particles were collected as water-droplets (Hwang and Ro, 2006).

Based on the morphological, X-ray spectral, and ATR-FT-IR spectral data, 109 individual particles were classified into different particle types, such as Ca-containing,  $\text{NaNO}_3$ -containing, silicates, and miscellaneous particles. Table S1 in the Supplement shows the chemical speciation results for all 109 particles determined by the combined use of the two techniques. The third and fourth columns of Table S1 list the elemental concentration and chemical species of each particle obtained from the low-Z particle EPMA data, respectively. Details pertaining to the low-Z particle EPMA data treatment and interpretation can be found in previous papers (Geng et al., 2009, 2010). The following gives a brief summary of how the particles were classified. Low-Z particle EPMA can provide quantitative information on the chemical composition. First, the particles were regarded to be composed of only one chemical species when the chemical species constituted at least a 90 % atomic fraction. Second, efforts were made to specify the chemical species, even for particles mixed internally with two or more chemical species. The mixed particles were specified based on all of chemical species with > 10 % in the formula fraction. Third, ED-EPMA has high detection limits of 0.1–1.0 %

## Observation of chemical modification of Asian Dust particles

Young-Chul Song et al.

[Title Page](#)[Abstract](#)[Introduction](#)[Conclusions](#)[References](#)[Tables](#)[Figures](#)[⏪](#)[⏩](#)[◀](#)[▶](#)[Back](#)[Close](#)[Full Screen / Esc](#)[Printer-friendly Version](#)[Interactive Discussion](#)

in weight due mainly to its high Bremsstrahlung background level. Therefore, elements with an atomic concentration less than 1.0% were not included in the chemical speciation procedure.

The ATR-FT-IR absorption peaks and chemical species obtained from the ATR-FT-IR spectral data are listed in the fifth and sixth columns of Table S1, respectively. The ATR-FT-IR spectral data was used qualitatively for molecular speciation and/or functional group analysis because of the difficulty in assessing molecular species of individual particles quantitatively using ATR-FT-IR spectral data when they are internal mixtures. A homemade ATR-FT-IR spectral library was initially consulted to specify the molecular species of individual particles using the ATR-FT-IR spectral data; inorganic compounds and minerals commonly encountered in airborne particle samples were measured by ATR-FT-IR to generate a custom ATR-FT-IR library (Jung et al., 2010; Malek et al., 2011). When the ATR-FT-IR spectrum of an individual particle was too complex to clearly specify all the chemical species of the particle, the IR absorption peaks were examined by functional group analysis based on the IR peak data available in the literature (Niemeyer et al., 1992; Allen et al., 1994; Cabaniss et al., 1998; Specht and Frimmel, 2001; Max and Chapados, 2004; Hay and Myneni, 2007; Hay and Myneni, 2007; Coury and Dillner, 2008). The seventh column of Table S1 lists the chemical species identified by the combined use of the two single-particle analytical techniques, which are the particle types used for the discussion.

Figure 2 shows an SEI obtained at higher magnification ( $\times 900$ ) than an overall SEI (Fig. 1a with  $\times 400$ ), where a more detailed morphology of the particles is shown together with their particle types. For the other particles, Figs. S1–S4 in the Supplement provide their SEIs obtained at higher magnification as well as their particle types. For the notation of particle types, a unique notation system was devised. A particle notated as  $(\text{Mg,Ca})(\text{NO}_3,\text{SO}_4)$  is an internal mixture of  $\text{Mg}(\text{NO}_3)_2$ ,  $\text{MgSO}_4$ ,  $\text{Ca}(\text{NO}_3)_2$ , and  $\text{CaSO}_4$  species. A particle denoted  $\text{cristobalite/Ca}(\text{CO}_3,\text{NO}_3)/\text{organic}/\text{H}_2\text{O}$  indicates that the particle is a mixture of cristobalite,  $\text{CaCO}_3$ ,  $\text{Ca}(\text{NO}_3)_2$ , and organic species, with the most abundant chemical species listed first. On the other hand, when water is

## Observation of chemical modification of Asian Dust particles

Young-Chul Song et al.

Title Page

Abstract

Introduction

Conclusions

References

Tables

Figures

⏪

⏩

◀

▶

Back

Close

Full Screen / Esc

Printer-friendly Version

Interactive Discussion



present in the particle, it is placed last just to indicate its presence. Among 109 particles, Ca-containing particles (41 particles; 38 %) were the most abundant, followed by  $\text{NaNO}_3$ -containing (33 particles; 30%), silicate (24 particles; 22%), and miscellaneous particles (11 particles; 10%).

### 3.1 Ca-containing particles

Among the 109 particles, the number of Ca-containing particles was 41, where just two particles are  $\text{CaCO}_3$  and the others are reacted (aged) ones containing  $\text{Ca}(\text{NO}_3)_2$ ,  $\text{CaSO}_4$ , or both, which are the reaction products of  $\text{CaCO}_3$  particles with  $\text{NO}_x/\text{HNO}_3$  and/or  $\text{SO}_x$ . Almost all Ca-containing particles (see particles #14, 17, 32, 42, 47, 49, 50, and 53 in Fig. 2) were collected as water droplets because they appear dark on their SEIs (Hwang and Ro, 2006). In addition, the presence of IR peaks of  $\text{H}_2\text{O}$  at 1620–1630 and 3300–3440  $\text{cm}^{-1}$  in their ATR-FT-IR spectra clearly shows that the dark particles contain water.

Figure 3 presents the ATR-FT-IR and X-ray spectral data and SEIs of the three typical Ca-containing particles. The ATR-FT-IR spectrum, X-ray spectrum and elemental atomic concentrations, and SEIs (taken before and after ATR-FT-IR imaging) of particle #89 are presented in Fig. 3a and d and the insets, respectively. Based on low-Z particle EPMA, its major elements were O (58 % in atomic fraction), C (23 %), Ca (12 %), Si (2 %), Al (1 %), S (1 %), Mg (1 %), and Fe (1 %), suggesting that particle #89 is a mixture of  $\text{CaCO}_3$  and carbonaceous species with minor content of aluminosilicate and sulfate. Its bright and angular SEI obtained before ATR-FT-IR imaging indicates its soil origin. The presence of the  $\text{CaCO}_3$  moiety in particle #89 was confirmed by the strong IR peaks from  $\text{CO}_3^{2-}$  of calcite at 872 and 1404  $\text{cm}^{-1}$  in its ATR-FT-IR spectrum, and its ATR-FT-IR spectral data clearly shows that the aluminosilicate moiety is montmorillonite due to its IR peaks at 790 and 1022  $\text{cm}^{-1}$  (Jung et al., 2010). Because the elemental concentrations of C and Ca are 23 % and 12 %, respectively, where 12 % C is combined with Ca, the remaining ~ 11 % carbon species appear to be IR-inactive

## Observation of chemical modification of Asian Dust particles

Young-Chul Song et al.

Title Page

Abstract

Introduction

Conclusions

References

Tables

Figures

⏪

⏩

◀

▶

Back

Close

Full Screen / Esc

Printer-friendly Version

Interactive Discussion



5 elemental carbon because no organic IR peak was observed. No IR peak for sulfate at  $1120\text{ cm}^{-1}$  was observed, even though the atomic concentration of sulfur by EPMA is significant ( $\sim 1\%$ ), suggesting that sulfate appears to be concentrated locally at the region where the X-rays were collected. The ATR-FT-IR spectrum provides information on the chemical species and functional groups of the particle, but a quantitative assessment of those species is still needed. The combined use of X-ray and ATR-FT-IR showed that particle #89 was a mixture of calcite, elemental carbon, and montmorillonite, and the majority of the particle was calcite. Only two calcite-rich particles did not experience aging during long-range transport, namely particles #3 and 89.

10 The ATR-FT-IR spectrum, X-ray spectrum and elemental atomic concentrations, and SEIs of particle #62 are presented in Fig. 3b and e and the insets, respectively. Low-Z particle EPMA revealed the major elements to be O (56%), C (21%), Ca (12%), N (9%), S (2%), and Cl (1%), suggesting that particle #62 is a mixture of  $\text{CaCO}_3$ , nitrate, and carbonaceous species with minor sulfate and chloride. Its dark and circular SEI indicates that it was collected as a water droplet. Indeed, the weak and broad IR absorption peak at  $\sim 3312\text{ cm}^{-1}$  was assigned to the water moiety. Naturally occurring  $\text{CaCO}_3$  can exist in six different forms, i.e. calcite, aragonite, vaterite, monohydrocalcite, and calcium carbonate hexahydrate, which are crystalline  $\text{CaCO}_3$  of a soil origin, and amorphous calcium carbonate (ACC) with a possible biogenic origin (Beniash et al., 1997; Addadi et al., 2003; Weiner et al., 2003). The six different  $\text{CaCO}_3$  forms were reported to have different IR spectra. In particular, ACC can be distinguished clearly from the crystalline  $\text{CaCO}_3$  forms because ACC shows two split peaks of the asymmetric stretching vibration due to the deficient symmetric environment of the  $\text{CO}_3^{2-}$  ion (Addadi et al., 2003; Weiner et al., 2003). As shown in Fig. 3b, particle #62 clearly shows two  $\text{CO}_3^{2-}$  peaks at  $1420$  and  $1484\text{ cm}^{-1}$ , which are characteristic for ACC. ACC can be emitted to the air from the skeletal components of various sea creatures (Addadi et al., 2003; Weiner et al., 2003). Therefore, these ACC particles might have been entrained when Asian Dust particles passed over the Yellow Sea. On the other hand, biogenic ACC in the skeletal components is not observed frequently in the atmospheric

**Observation of  
chemical  
modification of Asian  
Dust particles**

Young-Chul Song et al.

Title Page

Abstract

Introduction

Conclusions

References

Tables

Figures

⏪

⏩

◀

▶

Back

Close

Full Screen / Esc

Printer-friendly Version

Interactive Discussion



environment or even in nature. Among the 41 Ca-containing particles, four were ACC-rich particles, namely particles #57, 58, 62, and 63, which is a significant fraction. In addition, small and bright crystals inside dark particle #62 (see insets in Fig. 3) mainly contain Ca, C, and O elements in its X-ray spectrum (not shown), indicating that the small bright crystals were  $\text{CaCO}_3$ . The other three ACC particles except for particle #62 contained a small amount of silicate species (see Table S1 of Supplement), strongly suggesting their soil origin. Some carbonaceous species were organic because the IR peaks of the aliphatic CH group are present at 2865 and 2929  $\text{cm}^{-1}$ . In addition, the IR peak at 1630  $\text{cm}^{-1}$  was assigned to carboxylic ions ( $\text{COO}^-$ ) (Hay and Myneni, 2007), most likely from humic substances (Niemeyer et al., 1992) and/or organic compounds, such as oxygenated carboxylic carbonyl compounds (Russell et al., 2002). The IR peak at 1630–1640  $\text{cm}^{-1}$  can be from a water moiety, but water has also a stronger and broader peak at 3200–3400  $\text{cm}^{-1}$  than at 1630–1640  $\text{cm}^{-1}$ . Because the peak at  $\sim 1630 \text{ cm}^{-1}$  was stronger than that at  $\sim 3312 \text{ cm}^{-1}$ , it must be convoluted with the IR peak from carboxylic ions. The IR peak of nitrate at  $\sim 1350 \text{ cm}^{-1}$  was not observed because the carbonate peaks were too strong. On the other hand, the small peaks at 817 and 1120  $\text{cm}^{-1}$ , respectively, indicate that N and S elements detected by EPMA are in the forms of nitrate and sulfate, respectively. Although Cl was detected by EPMA, there was no IR peak related to this chloride species, most likely because it exists as IR-inactive  $\text{CaCl}_2$ . Through the combined use of X-ray and ATR-FT-IR spectral data, particle #62 was found to be a mixture of ACC, organic, nitrate, sulfate, and water, and the majority of the particle was ACC. The chemical modification of calcite into nitrates and sulfates during the long-range transport of Asian Dust particles has been reported extensively (Arimoto et al., 2004; Ro et al., 2005; Hwang and Ro, 2005, 2006; Sullivan et al., 2007a; Hwang et al., 2008; Geng et al., 2009). On the other hand, to the best of the authors' knowledge, this is the first report of airborne ACC particles observed in Asian Dust particle samples. Crystalline calcite particles cannot absorb water, but the observed ACC particles can be hygroscopic because they were collected as water

**Observation of  
chemical  
modification of Asian  
Dust particles**

Young-Chul Song et al.

Title Page

Abstract

Introduction

Conclusions

References

Tables

Figures

⏪

⏩

◀

▶

Back

Close

Full Screen / Esc

Printer-friendly Version

Interactive Discussion



droplets so that their radiative forcing and reactivity should be different from crystalline  $\text{CaCO}_3$  particles.

Three particles, namely particles #43, 48, and 52 (see their morphology in Fig. 2 and their elemental compositions in Table S1 of the Supplement), were  $\text{CaCl}_2$ -containing ones, which constitute a significant portion of Ca-containing particles. Their X-ray spectral data clearly show that  $\text{CaCl}_2$  is the major species with minor Mg, Al, and/or Si, and no IR peaks were observed because  $\text{CaCl}_2$  and  $\text{MgCl}_2$  are IR inactive. A few studies reported the chemical modification of  $\text{CaCO}_3$  mineral particles to  $\text{CaCl}_2$ , particularly in the marine boundary layer, where the HCl level is sufficiently high for their conversion (Sullivan et al., 2007b; Tobo et al., 2010). Although the Asian Dust sample was collected in Chuncheon, which is  $\sim 110$  km away from the coast, the  $\text{CaCl}_2$  particles must have been formed when Asian Dust passed over the Yellow Sea. This is the first report of the field observation of  $\text{CaCl}_2$  particles converted from  $\text{CaCO}_3$  in a sample collected in the planetary boundary layer.

Among the 41 Ca-containing particles, 32 particles experienced chemical modification through heterogeneous reactions of  $\text{CaCO}_3$  particles with  $\text{SO}_x/\text{H}_2\text{SO}_4$  and/or  $\text{NO}_x/\text{HNO}_3$  during long-range transport. As a typical example of such particles, the ATR-FT-IR spectrum, X-ray spectrum and elemental atomic concentrations, and SEIs of particle #50 are presented in Fig. 3c and f and the insets, respectively. Its major elements were O (61 %), C (14 %), Ca (10 %), N (7 %), and S (7 %), suggesting that particle #50 was a mixture of  $\text{CaCO}_3$ ,  $\text{Ca}(\text{NO}_3)_2$ ,  $\text{CaSO}_4$ , and carbonaceous species. Its dark and circular SEI indicates that it was collected as a water droplet, which is supported by the presence of IR absorption peaks at 1631 and  $\sim 3352\text{ cm}^{-1}$  from the water moiety. Some bright particles inside the dark region (see SEIs in insets of Fig. 3) would be crystalline  $\text{CaCO}_3$ . The presence of a strong IR peak at  $1120\text{ cm}^{-1}$  and sharp peaks at 814 and  $860\text{ cm}^{-1}$  confirmed the presence of  $\text{SO}_4^{2-}$ ,  $\text{NO}_3^-$ , and  $\text{CO}_3^{2-}$  moieties, respectively. The IR peaks characteristic for  $\text{NO}_3^-$  and  $\text{CO}_3^{2-}$  ions at 1375 and  $1394\text{ cm}^{-1}$ , respectively, were convoluted to a broad and asymmetric IR peak at  $\sim 1390\text{ cm}^{-1}$ . Some nitrate and sulfate most likely exists in acidic forms because the

**Observation of  
chemical  
modification of Asian  
Dust particles**

Young-Chul Song et al.

Title Page

Abstract

Introduction

Conclusions

References

Tables

Figures



Back

Close

Full Screen / Esc

Printer-friendly Version

Interactive Discussion



sum of the C, N, and S contents (24%) was larger than that of Ca (10%). Organic species were present, probably as humic substances of a soil origin and/or oxygenated carboxylic carbonyl compounds, due to the characteristic IR peak of carboxylic ions at  $1631\text{ cm}^{-1}$  (Hay and Myneni, 2007). Through the combined use of X-ray and ATR-FT-IR spectral data, particle #50 was found to be a mixture of  $\text{CaCO}_3$ ,  $\text{Ca}(\text{NO}_3)_2$ ,  $\text{CaSO}_4$ , organics, and water, and the major components of the particle were nitrates and sulfates including their acidic species. Among the 39 aged (reacted) Ca-containing particles, the number of particles containing nitrate, sulfate, and both were 10, 8, and 14, respectively, clearly showing that these Asian Dust particles had experienced extensive heterogeneous reactions during long-range transport.

### 3.2 $\text{NaNO}_3$ -containing particles

Among the 109 particles examined, 33 were  $\text{NaNO}_3$ -containing particles, which are the reaction products between sea-salt particles and  $\text{NO}_x/\text{HNO}_3$  (Laskin et al., 2002), with no observation of genuine sea-salt particles. As genuine sea-salt particles must have been entrained when Asian Dust particles passed over the Yellow Sea, the lack of genuine sea-salt particles indicates the facile formation of  $\text{NaNO}_3$  species through the heterogeneous reactions of sea-salts.

Among the 33  $\text{NaNO}_3$ -containing particles, 10 were crystalline. As a typical example, the ATR-FT-IR spectrum, X-ray spectrum and elemental atomic concentrations, and SEIs of particle #79 are presented in Fig. 4a and d and the insets, respectively. The major elements were O (54%), Na (24%), N (22%), and Ca (1%), suggesting that particle #79 is a  $\text{NaNO}_3$  particle. Its bright and cubic SEI indicates that it is a crystalline solid, which is supported by the absence of IR peaks of water. In addition, a sharp IR peak at  $1786\text{ cm}^{-1}$  is characteristic of crystalline  $\text{NaNO}_3$  species (Song et al., 2010). The ATR-FT-IR spectral data clearly supports that this is a  $\text{NaNO}_3$  particle because the IR peaks at 833, 1064, and  $1352\text{ cm}^{-1}$  are characteristic of  $\text{NO}_3^-$  ions. On the other hand, ATR-FT-IR provides additional information on the chemical species of this particle, i.e. nitrite species are also present due to an IR peak at  $1254\text{ cm}^{-1}$  of

## Observation of chemical modification of Asian Dust particles

Young-Chul Song et al.

Title Page

Abstract

Introduction

Conclusions

References

Tables

Figures



Back

Close

Full Screen / Esc

Printer-friendly Version

Interactive Discussion





**Observation of  
chemical  
modification of Asian  
Dust particles**

Young-Chul Song et al.

Title Page

Abstract

Introduction

Conclusions

References

Tables

Figures

⏪

⏩

◀

▶

Back

Close

Full Screen / Esc

Printer-friendly Version

Interactive Discussion

of  $\text{COO}^-$  at  $1561$  and  $1585\text{ cm}^{-1}$  and the weak peaks of aliphatic CH and carbonyl at  $\sim 2900\text{ cm}^{-1}$  (Allen et al., 1994; Coury and Dillner, 2008) and  $1690\text{ cm}^{-1}$  (Niemeyer et al., 1992; Max and Chapados, 2004), respectively. Although only N, O, and Na were detected in this particle by EPMA, this particle was divided into a few fragments, as shown in its SE image after ATR-FT-IR imaging (see the right inset in Fig. 4), which contained carbon, sulfur, and other elements by EPMA after ATR-FT-IR imaging. As the X-ray spectrum of particle #33 was obtained from the center of the particle before ATR-FT-IR imaging, only  $\text{NaNO}_3$  species was detected by low-Z particle EPMA, whereas the ATR-FT-IR signals were obtained from a large area, i.e.  $\sim 5.8\text{ }\mu\text{m}$  diameter (Jung et al., 2010), including the central  $\text{NaNO}_3$  and surrounding particles. The internally-mixed particles showed carbonyl and aliphatic CH peaks, which are probably humic substances from sea water.

Six  $\text{NaNO}_3$ -containing particles, such as particles #1, 8, 54, 66, 73, and 104 (see Table S1 of the Supplement), were internally mixed with silicate minerals. As an example, the ATR-FT-IR spectrum, X-ray spectrum and elemental atomic concentrations, and SEIs of particle #54 are presented in Fig. 4c and f and the insets, respectively. Its major elements were O (52%), N (23%), Na (17%), C (5%), and Ca (3%), suggesting that particle #33 is a  $\text{NaNO}_3$  particle with carbonaceous and Ca-containing species. The faint, dark circle surrounding bright crystalline particles, as observed on its SEI obtained before ATR-FT-IR imaging, indicates that it was collected as a water droplet containing  $\text{NaNO}_3$  species, which was confirmed by the presence of IR peaks of water at  $1634$  and  $\sim 3301\text{ cm}^{-1}$  and of crystalline  $\text{NaNO}_3$  at  $831$ ,  $1349$ , and  $1788\text{ cm}^{-1}$ . In addition, the ATR-FT-IR spectrum shows the presence of inorganic carbonate at  $862$  and  $1400\text{ cm}^{-1}$ , nitrite at  $1250\text{ cm}^{-1}$ , sulfate at  $1110\text{ cm}^{-1}$ , and montmorillonite at  $1013\text{ cm}^{-1}$ . These  $\text{NaNO}_3$ -containing particles mixed with silicate minerals, constituting a significant portion of  $\text{NaNO}_3$ -containing particles (i.e. 6 among overall 33 particles), appear to be due to coagulation between particles of marine and soil origins through cloud processing, which was also reported by other studies (Zhang et al., 2003; Sullivan et al., 2007b; Sobanska et al., 2012).

### 3.3 Silicate particles

Among the 109 particles examined, the number of silicate particles was 24, where 11, 8, 3, 2, 2, and 1 particle contain montmorillonite, quartz, feldspars, cristobalite, muscovite, and vermiculite, respectively. Although low-Z particle EPMA can provide the elemental concentrations to identify silicate particles, the speciation of silicate particles can be determined unambiguously by the combined use of their ATR-FT-IR spectral data (Jung et al., 2010). For this Asian Dust particle sample, the major silicates were montmorillonite and quartz. A previous study reported that montmorillonite and calcite are the characteristic, major silicates for Chinese loess soils, whereas quartz and feldspars are characteristic of Chinese desert soils (Malek et al., 2011).

Among 24 silicate particles, 14 particles were mineral particles without containing a considerable amount of water. As a typical example, the ATR-FT-IR spectrum, X-ray spectrum and elemental atomic concentrations, and SEIs of particle #24 are shown in Fig. 5a and d and the insets, respectively. Its major elements were O (60%), Si (15%), Al (14%), C (5%), K (3%), and Na (1%), suggesting that particle #24 is an aluminosilicate particle with carbonaceous species. Its bright and angular SEI before the ATR-FT-IR measurement indicates that it is a crystalline solid mineral. Based on its ATR-FT-IR spectral data, particle #24 was clearly identified as muscovite mixed internally with minor carbonate and organic species; i.e. IR peaks at 753, 821, 926, 1006, 1160, and 3630  $\text{cm}^{-1}$  are for muscovite (Jung et al., 2010), 1400  $\text{cm}^{-1}$  for carbonate, and  $\sim 1620 \text{ cm}^{-1}$  for carboxylic ion. The IR peak at 3630  $\text{cm}^{-1}$  was assigned to crystal OH in muscovite, and no water was present in this particle. During long-range transport, this silicate particle did not experience chemical modification. Among the 14 particles, seven particles contained swelling clay minerals, i.e. montmorillonite, and nine contained non-swelling quartz or muscovite.

Ten silicate particles were observed to contain nitrate, organic (possibly humic substances), and water, where five particles contain swelling clay minerals, such as montmorillonite and vermiculite, and the other five contained non-swelling minerals, such as

## Observation of chemical modification of Asian Dust particles

Young-Chul Song et al.

Title Page

Abstract

Introduction

Conclusions

References

Tables

Figures

⏪

⏩

◀

▶

Back

Close

Full Screen / Esc

Printer-friendly Version

Interactive Discussion



**Observation of  
chemical  
modification of Asian  
Dust particles**

Young-Chul Song et al.

[Title Page](#)[Abstract](#)[Introduction](#)[Conclusions](#)[References](#)[Tables](#)[Figures](#)[⏪](#)[⏩](#)[◀](#)[▶](#)[Back](#)[Close](#)[Full Screen / Esc](#)[Printer-friendly Version](#)[Interactive Discussion](#)

crystalite, quartz, and feldspar. The non-swelling silicate particles also contain water as well as nitrate and organic. As an example of swelling silicate particles containing nitrate, organic, and water, the ATR-FT-IR spectrum, X-ray spectrum and elemental atomic concentrations, and SEIs of particle #40 are shown in Fig. 5b and e and the insets, respectively. Its elemental concentrations were O (55 %), Si (10 %), C (12 %), N (7 %), Al (6 %), Ca (4 %), Mg (4 %), and Fe (2 %), suggesting that particle #40 is an aluminosilicate with nitrate and carbonaceous species. This particle was collected as a water droplet because its SEI before ATR-FT-IR imaging appeared dark and circular, and two crystalline particles were observed inside the dark circle. Based on its ATR-FT-IR spectral data, the major species of particle #40 is vermiculite supported by its IR peaks at 753, 833, 910, 1006, and 1158  $\text{cm}^{-1}$  (Jung et al., 2010), and minor components are carbonate (866 and 1404  $\text{cm}^{-1}$ ), nitrate (824 and 1367  $\text{cm}^{-1}$ ), water (1639 and 3305  $\text{cm}^{-1}$ ), and organics (1618  $\text{cm}^{-1}$  ( $\text{COO}^-$ ) and 1705  $\text{cm}^{-1}$  ( $\text{C}=\text{O}$ )). Vermiculite is one of the swelling clay minerals (Jung et al., 2010). This particle might have picked up water during long range transport, and nitrate was formed from the heterogeneous reaction of carbonate and  $\text{NO}_x/\text{HNO}_3$ . Water soluble organic species also appear to have been entrained in this particle during long-range transport.

As an example of non-swelling silicate particles containing nitrate, organic, and water, the ATR-FT-IR spectrum, X-ray spectrum and elemental atomic concentrations, and SEIs of particle #45 are shown in Fig. 5c and f and the insets, respectively. Its major elements were O (58 %), Si (20 %), Al (7 %), K (5 %), C (6 %), and N (2 %), suggesting that particle #40 is an aluminosilicate with carbonaceous and nitrate species. This particle was collected as a water droplet because its SEI showed a dark area surrounding an angular particle. ATR-FT-IR spectral data revealed the major species of particle #45 to be K-feldspar ( $\text{KAlSi}_3\text{O}_8$ ) supported by its IR peaks at 993, 1086, and 1109  $\text{cm}^{-1}$  (Jung et al., 2010) and the minor species to be carbonate (866 and 1410  $\text{cm}^{-1}$ ), water (1639 and 3314  $\text{cm}^{-1}$ ), and organic (1623  $\text{cm}^{-1}$  ( $\text{COO}^-$ )). As the atomic concentration of nitrogen was only 2 % based on X-ray analysis, the IR peak of nitrate appeared to be too small to be differentiated from carbonate peak.

**Observation of  
chemical  
modification of Asian  
Dust particles**

Young-Chul Song et al.

Title Page

Abstract

Introduction

Conclusions

References

Tables

Figures



Back

Close

Full Screen / Esc

Printer-friendly Version

Interactive Discussion



Only a few studies on the reactivity of silicate particles have been performed in laboratories. Of these, the major focus has been the ability of the adsorption and absorption of water by silicate particles because the water uptaken by silicate particles is believed to enhance the reactivity. Indeed, the water uptake was reported to be high for the swelling clay minerals (Frinak et al., 2005; Schuttlefield et al., 2007; Herich et al., 2009), and a swelling silicate mineral, i.e. Na-montmorillonite, can contain approximately 20 % water and 30 % HNO<sub>3</sub> by weight, even at 44 % RH (Mashburn et al., 2005). The current single-particle mineralogical field work, in which both the mineral types of silicate particles and the presence of water can be clearly identified, shows that the water uptake is not strongly dependent on the swelling property of the silicate minerals because some non-swelling silicates contain water, whereas some swelling minerals do not. In the present study, all water-containing, either swelling or non-swelling, silicate particles also contained a small amount of nitrate, carbonate, and organic components with the presence of calcium, strongly suggesting that the water uptake of Asian Dust silicate particles was governed by the original presence of CaCO<sub>3</sub> species in the silicate minerals (see Table S1 in the Supplement). In the laboratory, the water uptake and reactivity of pure swelling and/or non-swelling silicate particles were examined. The swelling minerals showed higher water uptake and reactivity. On the other hand, in this Asian Dust sample, the CaCO<sub>3</sub> moiety originally present in silicate mineral particles appears to be more important for their aging than their silicate mineral type. A previous study reported that many silicate particles of Chinese source soils were mixed internally with CaCO<sub>3</sub> (Malek et al., 2011). In particular, for the Chinese loess soils collected in Louchuan and Ganquan it was observed that more than 90 % of montmorillonite, muscovite, and illite contained carbonate minerals as their minor mineral, and more than 60 % of quartz, cristobalite, and feldspars did.

### 3.4 Miscellaneous particles

Eleven particles were classified as miscellaneous, which included four carbonaceous particles, two fly ash, two Mg-containing particles, two Fe-containing particles, and one aluminum oxide (see Table S1 in the Supplement).

The ATR-FT-IR spectrum, X-ray spectrum and elemental atomic concentrations, and SEIs of carbonaceous particles #6 and #31 are shown in Fig. 6a, b, d, and e and the insets, respectively. Particle #6 appeared dark and round on its SEI (Fig. 6d), indicating that it was collected as a water droplet. Its elemental concentrations based on X-ray analysis were C (34 %), N (36 %), O (26 %), S (3 %), and Cl (1 %), suggesting that it is a water-soluble organic aerosol (WSOA). Its ATR-FT-IR spectrum of particle #6 (Fig. 6a) revealed the presence of various types of functional groups, such as carbonyl carbon (C = O) at  $1727\text{ cm}^{-1}$ , carbon-carbon double bond (C = C) at  $1627\text{ cm}^{-1}$ , carboxylate ion ( $\text{COO}^-$ ) at  $1387$  and  $1552\text{ cm}^{-1}$ , organic nitrates ( $\text{CONO}_2$ ) or C-O-H bending at  $1244\text{ cm}^{-1}$ , C-O stretch at  $1035\text{ cm}^{-1}$ , ammonium ion ( $\text{NH}_4^+$ ) at  $1435$  and  $2850\text{--}3022\text{ cm}^{-1}$ , sulfate ( $\text{SO}_4^{2-}$ ) at  $965$  and  $1088\text{ cm}^{-1}$ , C-H at  $2967\text{ cm}^{-1}$ , and water at  $1630\text{--}1640$  and  $3324\text{ cm}^{-1}$ , indicating that particle #6 is a WSOA mixed with  $(\text{NH}_4)_2\text{SO}_4$ . As the content of nitrogen is much larger than that of sulfur, most of the nitrogen probably exists as organic nitrates. Particle #31 appeared dark and round with elemental concentrations of C (40 %), N (8 %), O (41 %), Na (4 %), S (4 %), and Ca (3 %) (Fig. 6e), indicating that it is also a WSOA. On the other hand, its ATR-FT-IR spectrum was different from that of particle #6 as shown in Fig. 6a and b. The ATR-FT-IR spectrum of particle #31 showed very strong aliphatic C-H IR absorption peaks at  $1442$ ,  $2857$ , and  $2922\text{ cm}^{-1}$  as well as strong C = O at  $1710\text{ cm}^{-1}$ ,  $\text{COO}^-$  at  $1367$  and  $1597\text{ cm}^{-1}$ , -C-OH at  $1166\text{ cm}^{-1}$ , and water  $3389\text{ cm}^{-1}$ . The two WSOAs should be differently-formed secondary organic aerosols by gas-to-particle conversion, but the combined use of X-ray and ATR-FT-IR spectral data could not clearly identify the organic molecular species even on a single particle basis. Among the four carbonaceous particles, particle #37 is also a WSOA, and particle #86 is elemental carbon because

## Observation of chemical modification of Asian Dust particles

Young-Chul Song et al.

Title Page

Abstract

Introduction

Conclusions

References

Tables

Figures

⏪

⏩

◀

▶

Back

Close

Full Screen / Esc

Printer-friendly Version

Interactive Discussion



its carbon content is largest based on X-ray analysis and no IR peak is detected in its ATR-FT-IR spectrum.

Two particles were observed as fly ash particles. For example, particle #71 appeared bright and circular. This is characteristic for fly ash particles generated during high temperature combustion processes. Its elemental concentrations based on X-ray analysis are C (2%), N (1%), O (63%), Al (12%), and Si (20%) and its ATR-FT-IR spectrum (Fig. 6c) shows silicate peaks (Si-O) at 826, 914, and 1014  $\text{cm}^{-1}$ , indicating that this is an aluminosilicate fly ash particle.

## 4 Conclusions

This study examined Asian Dust particles collected during an Asian Dust storm event on 11 November 2002 in Korea using low-Z particle EPMA and ATR-FT-IR imaging. Among the 109 particles analyzed, the most abundant particle type was Ca-containing one (38%), followed by  $\text{NaNO}_3$ -containing (30%), silicate (22%), and miscellaneous particles (10%). Among overall 41 Ca-containing particles, the number of particles containing nitrate, sulfate, both, ACC, and  $\text{CaCl}_2$  were 10, 8, 14, 4, and 3, respectively, whereas there were only two unreacted  $\text{CaCO}_3$  particles, clearly showing that the Asian Dust particles had experienced extensive heterogeneous reactions during long-range transport. In addition, a significant number of ACC particles were encountered in this Asian Dust sample for the first time, and the presence of  $\text{CaCl}_2$  particles converted from  $\text{CaCO}_3$  for the sample collected in the planetary boundary layer was also observed. Thirty three  $\text{NaNO}_3$ -containing particles, which are reaction products of sea-salt and  $\text{NO}_x/\text{HNO}_3$ , were observed, whereas no genuine sea-salt was encountered, indicating that sea-salt particles are more reactive than  $\text{CaCO}_3$  particles. Among the 24 silicate particles, 10 silicate particles, which is a significant fraction, including swelling minerals, such as montmorillonite and vermiculite, and non-swelling ones, such as feldspar and quartz, contained nitrate, organic, and water. The reactivity of silicate particles appear to be governed by the presence of internally mixed minor

## Observation of chemical modification of Asian Dust particles

Young-Chul Song et al.

Title Page

Abstract

Introduction

Conclusions

References

Tables

Figures

⏪

⏩

◀

▶

Back

Close

Full Screen / Esc

Printer-friendly Version

Interactive Discussion



CaCO<sub>3</sub> moiety, rather than the swelling property of silicate particles. This study provided detailed information on the physicochemical characteristics of individual Asian Dust particles, which experienced extensive chemical modification during long-range transport, through the combined use of two single-particle analytical techniques.

5 **Supplementary material related to this article is available online at:**  
**[http://www.atmos-chem-phys-discuss.net/12/27297/2012/  
acpd-12-27297-2012-supplement.pdf](http://www.atmos-chem-phys-discuss.net/12/27297/2012/acpd-12-27297-2012-supplement.pdf)**

*Acknowledgements.* This study was supported by Basic Science Research Programs through the National Research Foundation of Korea (NRF) funded by the Ministry of Education, Science, and Technology (Grant 2010-001881), and by Inha University. Also, we gratefully acknowledge support provided from National Natural Science Foundation of China (NSFC) grant 21177078 and the NSFC-NRF Scientific Cooperation Program (2012).

## References

- 15 Addadi, L., Raz, S., and Weiner, S.: Taking advantage of disorder: Amorphous Calcium Carbonate and its roles in biomineralization, *Adv. Mater.*, 15(12), 959–970, 2003.
- Allen, D. T., Palen, E. J., Haimov, M. I., Hering, S. V., and Young, J. R.: Fourier Transform Infrared Spectroscopy of Aerosol Collected in a Low Pressure Impactor (LPI/FTIR): Method Development and Field Calibration, *Aerosol Sci. Technol.*, 21, 325–342, 1994.
- 20 Allen, H. C., Mecartney, M. L., and Hemminger, J. C.: Minimizing Transmission Electron Microscopy Beam Damage during the Study of Surface Reactions on Sodium Chloride, *Microsc. Microanal.*, 4, 23–33, 1998.
- Andreae, M. O. and Rosenfeld, D.: Aerosol-cloud-precipitation interactions. Part 1. The nature and sources of cloud-active aerosols, *Earth-Sci. Rev.*, 89, 13–41, 2008.
- 25 Arimoto, R., Zhang, X. Y., Huebert, B. J., Kang, C. H., Savoie, D. L., Prospero, J. M., Sage, S. K., Schloesslin, C. A., Khaing, H. M., and Oh, S. N.: Chemical composition of atmospheric aerosols from Zhenbeitai, China, and Gosan, South Korea, during ACE-Asia, *J. Geophys. Res.*, 109, D19S04, doi:10.1029/2003JD004323, 2004.

**Observation of  
chemical  
modification of Asian  
Dust particles**

Young-Chul Song et al.

Title Page

Abstract

Introduction

Conclusions

References

Tables

Figures



Back

Close

Full Screen / Esc

Printer-friendly Version

Interactive Discussion



---

**Observation of  
chemical  
modification of Asian  
Dust particles**

---

Young-Chul Song et al.

---

[Title Page](#)[Abstract](#)[Introduction](#)[Conclusions](#)[References](#)[Tables](#)[Figures](#)[⏪](#)[⏩](#)[◀](#)[▶](#)[Back](#)[Close](#)[Full Screen / Esc](#)[Printer-friendly Version](#)[Interactive Discussion](#)

- Baker, A. R., Kelly, S. D., Biswas, K. F., Witt, M., and Jickells, T. D.: Atmospheric deposition of nutrients to the Atlantic Ocean, *Geophys. Res. Lett.*, 30, 2296–2299, 2003.
- Bergstrom, R. W., Pilewskie, P., Russell, P. B., Redemann, J., Bond, T. C., Quinn, P. K., and Sierau, B.: Spectral absorption properties of atmospheric aerosols, *Atmos. Chem. Phys.*, 7, 5937–5943, doi:10.5194/acp-7-5937-2007, 2007.
- Beniash, E., Aizenberg, J., Addadi, L., and Weiner, S.: Amorphous calcium carbonate transforms into calcite during sea urchin larval spicule growth, *Proc. R. Soc. Lond. B*, 461–465, 1997.
- Cabaniss, S. E., Leenheer, J. A., and McVey, I.F.: Aqueous infrared carboxylate absorbances: aliphatic di-acids, *Spectrochim. Acta A*, 54, 449–458, 1998.
- Chung, Y., Kim, H., Dulam, J., and Harris, J.: On heavy dustfall observed with explosive sandstorms in Chongwon-Chongju, Korea in 2002, *Atmos. Environ.*, 37, 3425–3433, 2003.
- Cohen, D. D., Garton, D., Stelcer, E., Hawas, O., Wang, T., Poon, S., Kim, J., Choi, B. C., Oh, S. N., Shin, H. J., Ko, M. Y., and Uematsu, M.: Multielemental analysis and characterization of fine aerosols at several key ACE-Asia sites, *J. Geophys. Res.*, 109, D19S12, doi:10.1029/2003JD003569, 2004.
- Coury, C. and Dillner, A. M.: A method to quantify organic functional groups and inorganic compounds in ambient aerosols using attenuated total reflectance FT-IR spectroscopy and multivariate chemometric techniques, *Atmos. Environ.*, 5923–5932, 2008.
- Fairlie, T. D., Jacob, D. J., and Park, R. J.: The impact of transpacific transport of mineral dust in the United States, *Atmos. Environ.*, 41, 1251–1266, 2007.
- Frinak, E. K., Mashburn, C. D., Tolbert, M. A., and Toon, O. B.: Infrared characterization of water uptake by low-temperature Na-montmorillonite: Implications for Earth and Mars, *J. Geophys. Res.*, 110, D09308, doi:10.1029/2004JD005647, 2005.
- Geng, H., Park, Y., Hwang, H., Kang, S., and Ro, C.-U.: Elevated nitrogen-containing particles observed in Asian dust aerosol samples collected at the marine boundary layer of the Bohai Sea and the Yellow Sea, *Atmos. Chem. Phys.*, 9, 6933–6947, doi:10.5194/acp-9-6933-2009, 2009.
- Geng, H., Kang, S., Choel, M., Kim, H., and Ro, C.-U.: Characterization of submicron aerosol particles collected in Incheon, Korea by quantitative TEM-EDX individual particle analysis, *J. Geophys. Res.*, 115, D15306, doi:10.1029/2009JD013486, 2010.

**Observation of  
chemical  
modification of Asian  
Dust particles**

Young-Chul Song et al.

Title Page

Abstract

Introduction

Conclusions

References

Tables

Figures

⏪

⏩

◀

▶

Back

Close

Full Screen / Esc

Printer-friendly Version

Interactive Discussion



Goldstein, J. I., Newbury, D. E., Joy, D. C., Lyman, C., Echlin, P., Lifshin, E., Sawyer, L., and Michael, J.: Scanning Electron Microscopy and X-ray Microanalysis, 3rd Edn., Kluwer-Plenum, New York, 2003.

Griffiths, P. R. and de Haseth, J. A.: Fourier Transform Infrared Spectrometry, 2 Edn., John Wiley & Sons, Inc., Hoboken, New Jersey, 2007.

Hay, M. B. and Myneni, S. C. B.: Structural environments of carboxyl groups in natural organic molecules from terrestrial systems. Part 1: Infrared spectroscopy, *Geochim. Cosmochim. Acta*, 71, 3518–3532, 2007.

Herich, H., Tritscher, T., Wiacek, A., Gysel, M., Weingartner, E., Lohmann, U., Baltensperger, U., and Cziczo D. J.: Water uptake of clay and desert dust aerosol particles at sub- and supersaturated water vapor conditions, *Phys. Chem. Chem. Phys.*, 11, 7804–7809, 2009.

Huebert, B. J., Bates, T., Russell, P. B., Shi, G. Y., Kim, Y. J., Kawamura, K., Carmichael, G., and Nakajima, T.: An overview of ACE-Asia: Strategies for quantifying the relationships between Asian aerosols and their climatic impacts, *J. Geophys. Res.*, 108, 8633–8652, 2003.

Hwang, H. and Ro, C.-U.: Single-particle characterization of four aerosol samples collected in Chuncheon, Korea, during Asian dust storm events in 2002, *J. Geophys. Res.*, 110, D23201, doi:10.1029/2005JD006050, 2005.

Hwang, H. and Ro, C.-U.: Direct observation of nitrate and sulfate formations from mineral dust and sea-salts using low-Z particle EPMA, *Atmos. Environ.*, 40, 3869–3880, 2006.

Hwang, H., Kim, H., and Ro, C.-U.: Single-particle characterization of aerosol samples collected before and during an Asian dust storm in Chuncheon, Korea, *Atmos. Environ.*, 42, 8738–8746, 2008.

Jung, H., Malek, M. A., Ryu, J., Kim, B., Song, Y., Kim, H., and Ro, C.-U.: Speciation of Individual Mineral Particles of Micrometer Size by the Combined Use of Attenuated Total Reflectance-Fourier Transform-Infrared Imaging and Quantitative Energy-Dispersive Electron Probe X-ray Microanalysis Techniques, *Anal. Chem.*, 82, 6193–6202, 2010.

Kim, H. and Ro, C.-U.: Characterization of Individual Atmospheric Aerosols Using Quantitative Energy Dispersive-Electron Probe X-ray Microanalysis: A Review, *Asian J. Atmos. Environ.*, 4, 115–140, 2010.

Laskin A., Iedema M. J., and Cowin, J. P.: Quantitative time-resolved monitoring of nitrate formation in sea salt particles using a CCSEM/EDX single particle analysis, *Environ. Sci. Technol.*, 36, 4948–4955, 2002.

**Observation of  
chemical  
modification of Asian  
Dust particles**

Young-Chul Song et al.

Title Page

Abstract

Introduction

Conclusions

References

Tables

Figures

⏪

⏩

◀

▶

Back

Close

Full Screen / Esc

Printer-friendly Version

Interactive Discussion



Laskin, A., Wietsma, T. W., Krueger, B. J., and Grassian, V. H.: Heterogeneous chemistry of individual mineral dust particles with nitric acid: A combined CCSEM/EDX, ESEM, and ICP-MS study, *J. Geophys. Res.*, 110, D10208, doi:10.1029/2004JD005206, 2005.

Li-Jones, X., Maring, H. B., and Prospero, J. M.: Effect of relative humidity on light scattering by mineral dust aerosol as measured in the marine boundary layer over the tropical Atlantic Ocean, *J. Geophys. Res.*, 103, 31113–31121, 1998.

Malek, M. A., Kim, B., Jung, H., Song, Y., and Ro, C.-U.: Single-particle mineralogy of Chinese soil particles by the combined use of low-Z particle electron probe X-ray microanalysis and attenuated total reflectance-FT-IR imaging techniques, *Anal. Chem.*, 83, 7970–7977, 2011.

Manktelow, P. T., Carslaw, K. S., Mann, G. W., and Spracklen, D. V.: The impact of dust on sulfate aerosol, CN and CCN during an East Asian dust storm, *Atmos. Chem. Phys.*, 10, 365–382, doi:10.5194/acp-10-365-2010, 2010.

Mashburn, C. D., Frinak, E. K., and Tolbert, M. A.: Heterogeneous uptake of nitric acid on Na-montmorillonite clay as a function of relative humidity, *J. Geophys. Res.*, 111, D15213, doi:10.1029/2005JD006525, 2006.

Maskey, S., Geng, H., Song, Y.-C., Hwang, H., Yoon, Y., Ahn, K.-H., and Ro, C.-U.: Single-particle characterization of summertime Antarctic aerosols collected at King George Island using quantitative energy-dispersive electron probe X-ray microanalysis and attenuated total reflection Fourier transform-infrared imaging techniques, *Environ. Sci. Technol.*, 45, 6275–6282, 2011.

Max, J. J. and Chapados, C.: Infrared Spectroscopy of Aqueous Carboxylic Acids: Comparison between Different Acids and Their Salts, *J. Phys. Chem. A*, 108, 3324–3337, 2004.

Maxwell-Meier, K., Weber, R., Song, C., Orsini, D., Ma, Y., Carmichael, G. R., and Streets, D. G.: Inorganic composition of fine particles in mixed mineral dust-pollution plumes observed from airborne measurements during ACE-Asia, *J. Geophys. Res.*, 109, D19S07, doi:10.1029/2003JD004464, 2004.

McNaughton, C. S., Clarke, A. D., Howell, S. G., Moore, K. G., Brekhovskikh, V., Weber, R. J., Orsini, D. A., Covert, D. S., Buzorius, G., Brechtel, F. J., Carmichael, G. R., Tang, Y. H., Eisele, F. L., Mauldin, R. L., Bandy, A. R., Thornton, D. C., and Blomquist, B.: Spatial distribution and size evolution of particles in Asian outflow: Significance of primary and secondary aerosols during ACE-Asia and TRACE-P, *J. Geophys. Res.*, 109, D19S06, doi:10.1029/2003JD003528, 2004.

## Observation of chemical modification of Asian Dust particles

Young-Chul Song et al.

Title Page

Abstract

Introduction

Conclusions

References

Tables

Figures

⏪

⏩

◀

▶

Back

Close

Full Screen / Esc

Printer-friendly Version

Interactive Discussion



Niemeyer, J., Chen, Y., and Bollag, J.-M.: Characterization of Humic Acids, Composts, and Peat by Diffuse Reflectance Fourier-Transform Infrared Spectroscopy, *Soil Sci. Soc. Am. J.*, 56, 135–140, 1992.

Paytan, A., Mackey, K. R. M., Chen, Y., Lima, I. D., Doney, S. C., Mahowald, N., Labiosa, R., and Post, A. F.: Toxicity of atmospheric aerosols on marine phytoplankton, *Proc. Natl. Acad. Sci. USA*, 106, 4601–4605, 2009.

Price, H. U., Jaffe, D. A., Cooper, O. R., and Doskey, P. V.: Photochemistry, ozone production, and dilution during long-range transport episodes from Eurasia to the northwest United States, *J. Geophys. Res.*, 109, D23S13, doi:10.1029/2003JD004328, 2004.

Ro, C.-U., Osan, J., and Van Grieken, R.: Determination of Low-Z Elements in Individual Environmental Particles Using Windowless EPMA, *Anal. Chem.*, 71, 1521–1528, 1999.

Ro, C.-U., Osan, J., Szaloki, I., Oh, K. Y., Kim, H., and Van Grieken, R.: Determination of Chemical Species in Individual Aerosol Particles Using Ultra-thin Window EPMA, *Environ. Sci. Technol.*, 34, 3023–3030, 2000.

Ro, C.-U., Oh, K.-Y., Kim, H., Chun, Y.-S., Osan, J., de Hoog, J., and Van Grieken, R.: Chemical speciation of individual atmospheric particles using low-Z electron probe X-ray microanalysis: characterizing “Asian Dust” deposited with rainwater in Seoul, Korea, *Atmos. Environ.* 35, 4995–5005, 2001.

Ro, C.-U., Osan, J., Szaloki, I., de Hoog, J., Worobiec, A., and Van Grieken, R.: A Monte Carlo Program for Quantitative Electron-induced X-ray Analysis of Individual Particles, *Anal. Chem.*, 75, 851–859, 2003.

Ro, C.-U., Kim, H., and Van Grieken, R.: An Expert System for Chemical Speciation of Individual Particles Using Low-Z Particle Electron Probe X-ray Microanalysis Data, *Anal. Chem.*, 76, 1322–1327, 2004.

Ro, C.-U., Hwang, H., Kim, H., Chun, Y., and Van Grieken, R.: Single-Particle Characterization of Four Asian Dust Samples Collected in Korea, Using Low-Z Particle Electron Probe X-ray Microanalysis, *Environ. Sci. Technol.*, 39, 1409–1419, 2005.

Roca, M., Zahardis, J., Bone, J., El-Maazawi, M., and Grassian, V. H.: 310 nm Irradiation of Atmospherically Relevant Concentrated Aqueous Nitrate Solutions: Nitrate Production and Quantum Yields, *J. Phys. Chem. A*, 112, 13275–13281, 2008.

Russell, L. M., Maria, S. F., and Myneni, S. C. B.: Mapping organic coatings on atmospheric particles, *Geophys. Res. Lett.*, 29, 1779, doi:10.1029/2002GL014874, 2002.

**Observation of  
chemical  
modification of Asian  
Dust particles**

Young-Chul Song et al.

Title Page

Abstract

Introduction

Conclusions

References

Tables

Figures

◀

▶

◀

▶

Back

Close

Full Screen / Esc

Printer-friendly Version

Interactive Discussion



- Ryu, J. and Ro, C.-U.: ATR-FT-IR Imaging and Quantitative ED-EPMA Techniques for Single Particle Analysis of Atmospheric Aerosol Particles, *Anal. Chem.*, 81, 6695–6707, 2009.
- Schuttlefield, J. D., Cox, D., and Grassian, V. H.: An investigation of water uptake on clays minerals using ATR-FTIR spectroscopy coupled with quartz crystal microbalance measurements, *J. Geophys. Res.*, 112, D21303, doi:10.1029/2007JD008973, 2007.
- 5 Sobanska, S., Hwang, H., Choël, M., Jung, H.-J., Eom, H.-J., Kim, H., Barbillat, J., and C.-U. Ro: Investigation of the Chemical Mixing State of Individual Asian Dust Particles by the Combined Use of Electron Probe X-ray Microanalysis and Raman Microspectrometry, *Anal. Chem.*, 84, 3145–3154, 2012.
- 10 Song, Y., Ryu, J., Malek, M. A., Jung, H., and Ro, C.-U.: Chemical speciation of individual airborne particles by the combined use of quantitative energy-dispersive electron probe X-ray microanalysis and attenuated total reflection Fourier transform-infrared imaging techniques, *Anal. Chem.*, 82, 7987–7998, 2010.
- 15 Specht, C. H. and Frimmel, F. H.: An in situ ATR-FT-IR study on the adsorption of dicarboxylic acids onto kaolinite in aqueous suspensions, *Phys. Chem. Chem. Phys.*, 3, 5444–5449, 2001.
- Sullivan, R. C., Guazzotti, S. A., Sodeman, D. A., and Prather, K. A.: Direct observations of the atmospheric processing of Asian mineral dust, *Atmos. Chem. Phys.*, 7, 1213–1236, doi:10.5194/acp-7-1213-2007, 2007a.
- 20 Sullivan, R. C., Guazzotti, S. A., Sodeman, D. A., Tang, Y., Carmichael, G. R., and Prather, K. A.: Mineral dust is a sink for chlorine in the marine boundary layer, *Atmos. Environ.*, 41, 7166–7179, 2007b.
- Thornton, J. A., Kercher, J. P., Riedel, T. P., Wagner, N. L., Cozic, J., Holloway, J. S., Dube, W. P., Wolfe, G. M., Quinn, P. K., Middlebrook, A. M., Alexander, B., and Steven S. B.: A large atomic chlorine source inferred from mid-continental reactive nitrogen chemistry, *Nature*, 464, 271–274, 2010.
- 25 Tobo, Y., Zhang, D., Matsuki, A., and Iwasaka, Y.: Asian dust particles converted into aqueous droplets under remote marine atmospheric conditions, *Proc. Natl. Acad. Sci. USA*, 96, 3396–3403, 2010.
- 30 Uno, I., Eguchi, K., Yumimoto, K., Takemura, T., Shimizu, A., Uematsu, M., Liu, Z. Y., Wang, Z., Hara, Y., and Sugimoto, N.: Asian dust transported one full circuit around the globe, *Nat. Geosci.*, 2, 557–560, 2009.

---

**Observation of  
chemical  
modification of Asian  
Dust particles**Young-Chul Song et al.

---

[Title Page](#)[Abstract](#)[Introduction](#)[Conclusions](#)[References](#)[Tables](#)[Figures](#)[⏪](#)[⏩](#)[◀](#)[▶](#)[Back](#)[Close](#)[Full Screen / Esc](#)[Printer-friendly Version](#)[Interactive Discussion](#)

- Vekemans, B., Janssens, K., Vincze, L., Adams, F., and Van Espen, P.: Analysis of X-ray spectra by iterative least squares (AXIL): New developments, *X-Ray Spectrom.*, 23, 278–285, 1994.
- Weiner, S., Kalisman, Y. L., Raz, S., and Addadi, L.: Biologically Formed Amorphous Calcium Carbonate, *Conn. Tiss. Res.*, 44, 214–218, 2003.
- 5 Worobiec, A., de Hoog, J., Osan, J., Szaloki, I., Ro, C.-U., and Van Grieken, R.: Thermal stability of beam sensitive atmospheric particles in electron probe microanalysis at liquid nitrogen temperature, *Spectrochim. Acta B*, 58, 851–865, 2003.
- Xu, J., Bergin, M. H., Greenwald, R., Schauer, J. J., Shafer, M. M., Jaffrezo, J. L., and Aymoz, G.: Aerosol chemical, physical, and radiative characteristics near a desert
- 10 source region of northwest China during ACE-Asia, *J. Geophys. Res.*, 109, D19S03, doi:10.1029/2003JD004239, 2004.
- Zhang, D. Z., Iwasaka, Y., Shi, G. Y., Zang, J. Y., Matsuki, A., and Trochkin, D.: Mixture state and size of Asian dust particles collected at southwestern Japan in spring 2000, *J. Geophys. Res.* 108, 4760–4771, 2003.
- 15 Ziemba, L. D., Dibb, J. E., Griffin, R. J., Anderson, C. H., Whitlow, S. I., Lefer, B. L., Rappengluck, B., and Flynn, J.: Heterogeneous conversion of nitric acid to nitrous acid on the surface of primary organic aerosol in an urban atmosphere, *Atmos. Environ.*, 44, 4081–4089, 2010.

**Observation of  
chemical  
modification of Asian  
Dust particles**

Young-Chul Song et al.

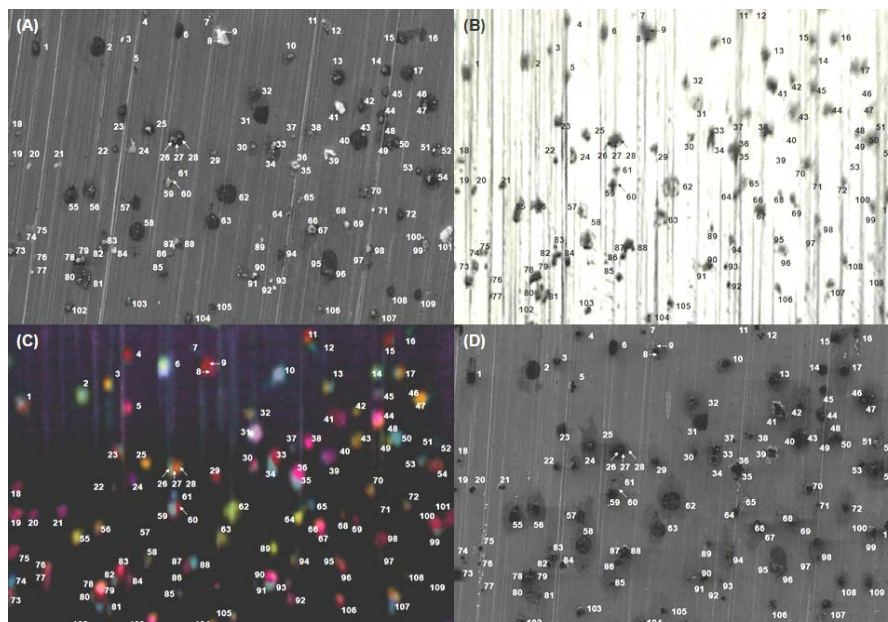


**Fig. 1.** (A) Secondary electron image (SEI) before the ATR-FT-IR imaging measurements, (B) visible light optical image, (C) ATR-FT-IR image, and (D) SEI after the ATR-FT-IR imaging of the same 109 individual airborne particles on Ag foil.

[Title Page](#)[Abstract](#)[Introduction](#)[Conclusions](#)[References](#)[Tables](#)[Figures](#)[⏪](#)[⏩](#)[◀](#)[▶](#)[Back](#)[Close](#)[Full Screen / Esc](#)[Printer-friendly Version](#)[Interactive Discussion](#)

## Observation of chemical modification of Asian Dust particles

Young-Chul Song et al.

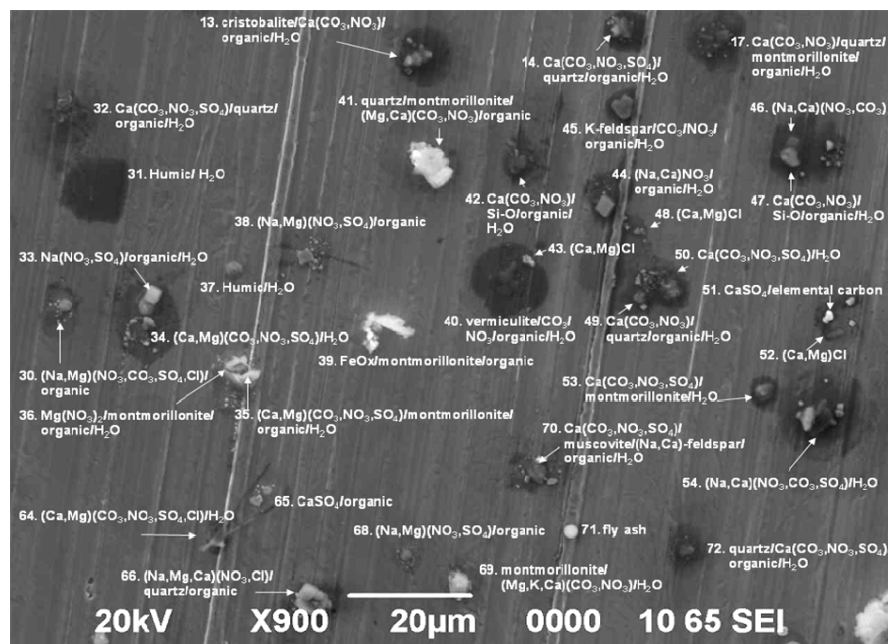


**Fig. 2.** An SEI obtained in a higher magnification than the overall SEI shown in Fig. 1.

Title Page

Abstract

Introduction

Conclusions

References

Tables

Figures

⏪

⏩

◀

▶

Back

Close

Full Screen / Esc

Printer-friendly Version

Interactive Discussion

## Observation of chemical modification of Asian Dust particles

Young-Chul Song et al.

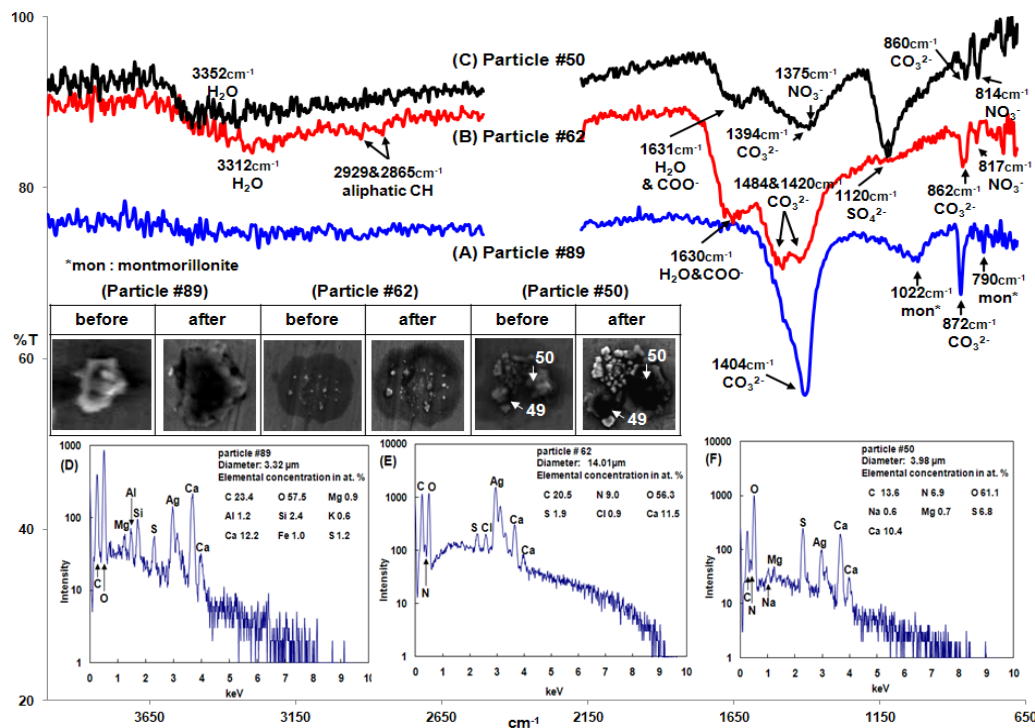


**Fig. 3.** ATR-FT-IR and X-ray spectra of typical Ca-containing particles and SEIs of particles obtained before and after the ATR-FT-IR imaging. The data for the 2200–2530  $\text{cm}^{-1}$  region where atmospheric  $\text{CO}_2$  peaks are present was deleted for clarity.

Title Page

Abstract

Introduction

Conclusions

References

Tables

Figures

◀

▶

◀

▶

Back

Close

Full Screen / Esc

Printer-friendly Version

Interactive Discussion

## Observation of chemical modification of Asian Dust particles

Young-Chul Song et al.

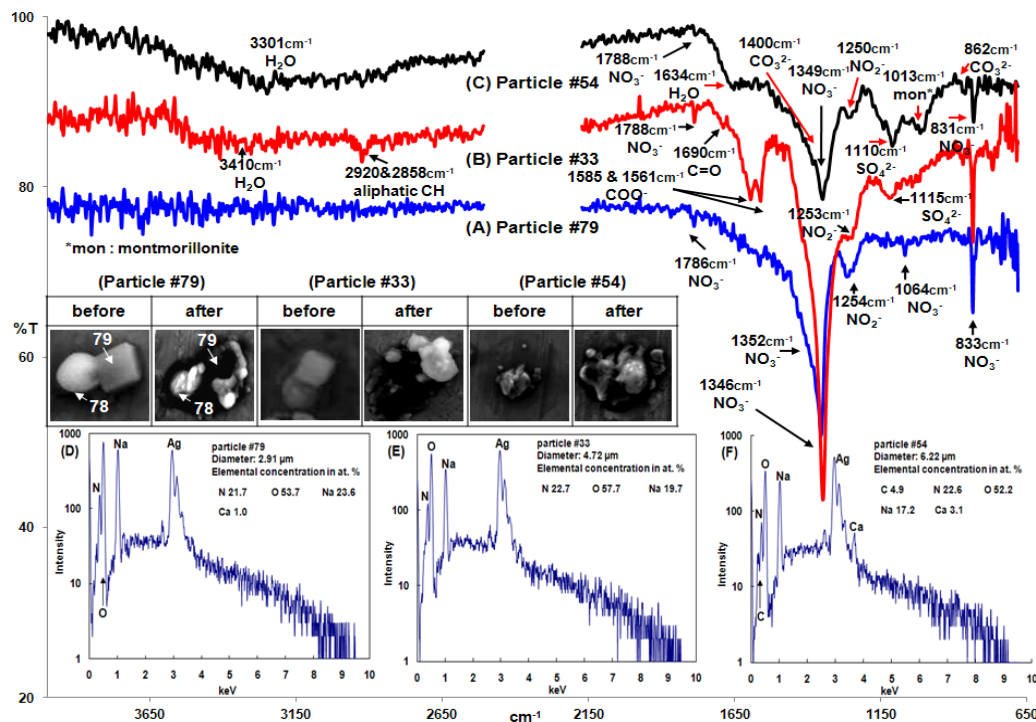


**Fig. 4.** ATR-FT-IR and X-ray spectra of typical  $\text{NaNO}_3$ -containing particles and SEIs of particles obtained before and after ATR-FT-IR imaging. The data for the  $2200\text{--}2530\text{cm}^{-1}$  region where atmospheric  $\text{CO}_2$  peaks are present was deleted for clarity.

Title Page

Abstract

Introduction

Conclusions

References

Tables

Figures

◀

▶

◀

▶

Back

Close

Full Screen / Esc

Printer-friendly Version

Interactive Discussion

## Observation of chemical modification of Asian Dust particles

Young-Chul Song et al.

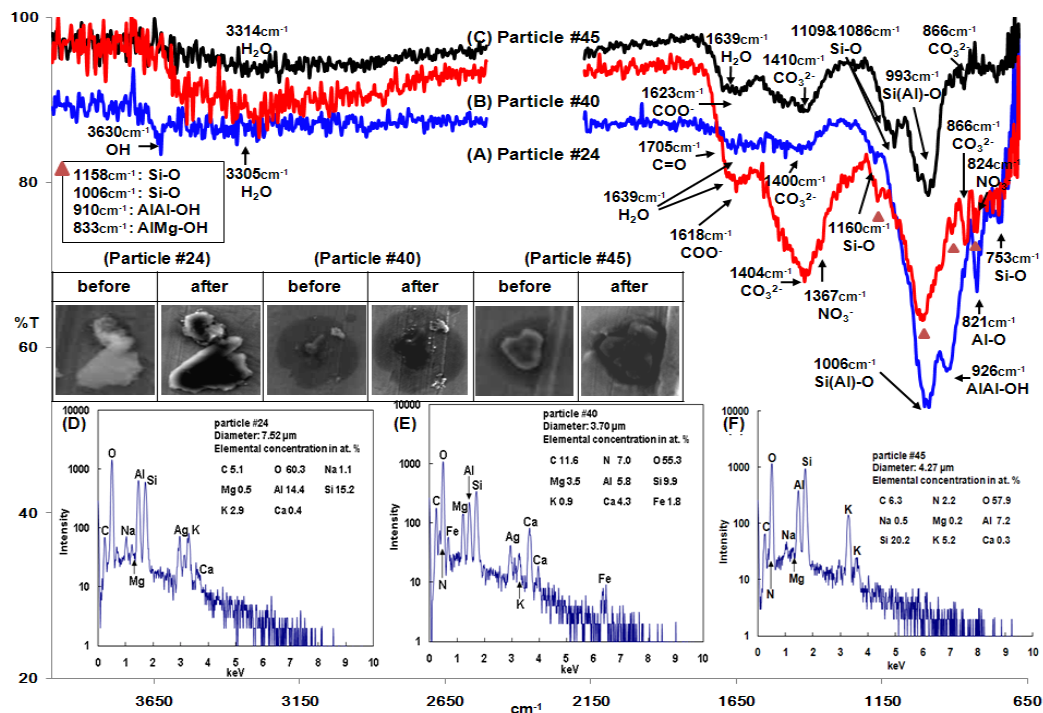


**Fig. 5.** ATR-FT-IR and X-ray spectra of typical silicate particles and SEIs of particles obtained before and after ATR-FT-IR imaging. The data for the 2200–2530 cm<sup>-1</sup> region where atmospheric CO<sub>2</sub> peaks are present was deleted for clarity.

[Title Page](#)
[Abstract](#)
[Introduction](#)
[Conclusions](#)
[References](#)
[Tables](#)
[Figures](#)
[Back](#)
[Close](#)
[Full Screen / Esc](#)
[Printer-friendly Version](#)
[Interactive Discussion](#)

## Observation of chemical modification of Asian Dust particles

Young-Chul Song et al.

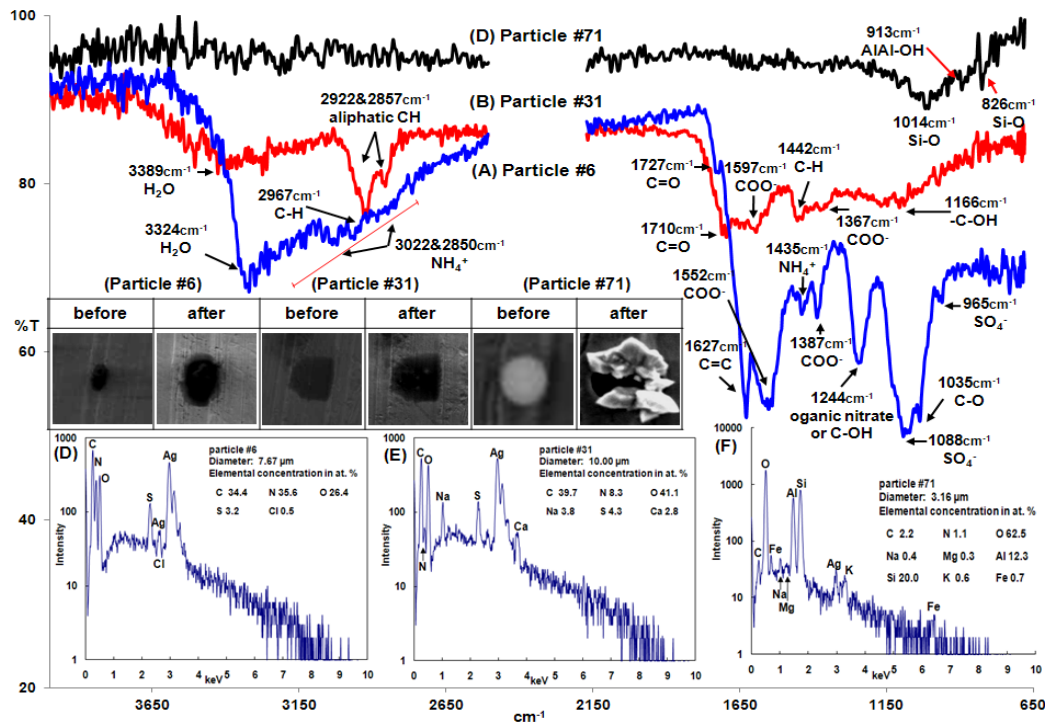


**Fig. 6.** ATR-FT-IR and X-ray spectra of miscellaneous particles and SEIs of particles obtained before and after ATR-FT-IR imaging. The data for the 2200–2530 cm<sup>-1</sup> region where atmospheric CO<sub>2</sub> peaks are present was deleted for clarity.

[Title Page](#)
[Abstract](#)
[Introduction](#)
[Conclusions](#)
[References](#)
[Tables](#)
[Figures](#)
[Back](#)
[Close](#)
[Full Screen / Esc](#)
[Printer-friendly Version](#)
[Interactive Discussion](#)